PROTEINS
STRUCTURE ■ FUNCTION ■ BIOINFORMATICS

Thermal stabilization of the protozoan *Entamoeba histolytica* alcohol dehydrogenase by a single proline substitution

Edi Goihberg,[1] Orly Dym,[2,3] Shoshana Tel-Or,[1] Linda Shimon,[4] Felix Frolow,[5,6] Moshe Peretz,[1] and Yigal Burstein[1]*

[1] Department of Organic Chemistry, Weizmann Institute of Science, Rehovot 76100, Israel
[2] Department of Structural Biology, Weizmann Institute of Science, Rehovot 76100, Israel
[3] Israel Structural Proteomics Center (ISPC), Weizmann Institute of Science, Rehovot 76100, Israel
[4] Chemical Research Support, Weizmann Institute of Science, Rehovot 76100, Israel
[5] Department of Molecular Microbiology and Biotechnology, The George S. Wise Faculty of Life Sciences, Tel-Aviv University, Ramat Aviv 69978, Israel
[6] The Daniella Rich Institute for Structural Biology, Tel-Aviv University, Ramat Aviv 69978, Israel

ABSTRACT

Analysis of the three-dimensional structures of two closely related thermophilic and hyperthermophilic alcohol dehydrogenases (ADHs) from the respective microorganisms Entamoeba histolytica (EhADH1) and Thermoanaerobacter brockii (TbADH) suggested that a unique, strategically located proline residue (Pro275) at the center of the dimerization interface might be crucial for maintaining the thermal stability of TbADH. To assess the contribution of Pro275 to the thermal stability of the ADHs, we applied site-directed mutagenesis to replace Asp275 of EhADH1 with Pro (D275P-EhADH1) and conversely Pro275 of TbADH with Asp (P275D-TbADH). The results indicate that replacing Asp275 with Pro significantly enhances the thermal stability of EhADH1 ($\Delta T_{1/2} \leq +10^{\circ}C$), whereas the reverse mutation in the thermophilic TbADH (P275D-TbADH) reduces the thermostability of the enzyme ($\Delta T_{1/2} \leq -18.8^{\circ}C$). Analysis of the crystal structures of the thermostabilized mutant D275P-EhADH1 and the thermocompromised mutant P275D-TbADH suggest that a proline residue at position 275 thermostabilized the enzymes by reducing flexibility and by reinforcing hydrophobic interactions at the dimer–dimer interface of the tetrameric ADHs.

Proteins 2008; 72:711–719.

Key words: thermal stability; site-directed mutagenesis; protozoan parasite; X-ray crystallography; hydrophobic interactions; intersubunit associations.

INTRODUCTION

The stabilization of biocatalysts is of great economic interest.[1] Understanding the mechanisms of protein thermal stability (kinetic stability) and thermostability (thermodynamic stability) is important because of their involvement in protein folding,[1,2] yet the forces regulating protein stability toward elevated temperatures are not completely resolved.[3]

Several mechanisms have been shown to contribute to the thermal stability of proteins, such as: decreasing flexibility and increasing rigidity, achieved by amino acid substitutions that increase hydrophobicity, stabilizing dipole moments of α-helices, shortening and deleting exposed loops, increasing intersubunit contacts by enhancing the hydrophobic effect, and decreasing the entropy of the unfolded state by the strategic placement of prolines.[4,5]

Multiple studies indicate that intersubunit associations play a major role in stabilizing oligomeric proteins. For instance, Kelly and coworkers demonstrated that the integrity of the quaternary structure of the human transthyterin molecule is a prerequisite for the maintenance of the soluble and stable form of the protein, which otherwise is transformed into amyloidogenic form when the quaternary structure is hampered by naturally occurring mutations.[6] Mitra *et al.* studied the stability of two dimeric legume lectins Concavalin A and WBAII, and concluded that the superior stability of Concavalin A could, to a major extent, be assigned to a higher degree of intersubunit associations.[7] Similarly Bjork *et al.* demonstrated that the thermal stability of tetrameric malate dehydrogenase from the bacterium *Chloflexus aurantiacus* could be achieved following the introduction of a single disulfide bridge at the dimer–dimer interface.[8] In accordance

Grant sponsor: Israel Science Foundation; Grant number: 296-00.
*Correspondence to: Dr. Yigal Burstein, Department of Organic Chemistry, Weizmann Institute of Science, 76100 Rehovot, Israel. E-mail: yigal.burstein@weizmann.ac.il
Received 27 April 2007; Revised 28 November 2007; Accepted 3 December 2007
Published online 7 February 2008 in Wiley InterScience (www.interscience.wiley.com).
DOI: 10.1002/prot.21946

with this finding, Nakka *et al.* showed that the disruption of the disulfide bridge at the dimerization interface of the glucose-6-phosphate dehydrogenase from the hyperthermophilic bacterium *Aquifex aeolicus* dramatically decreased the thermostability of the enzyme.[9] Conversely, Stroppolo *et al.* found that the difference in the stability between human Cu/Zn superoxide dismutase and the prokaryotic Cu,Zn SOD from *P. leiognathi* is due to the different stabilities of the individual monomers rather than in different stabilities of the quaternary structures.[10]

In the alcohol dehydrogenases (ADHs), intersubunit interactions have been proposed to contribute significantly to the stability the enzymes.[11–13] A study of the mesophile *Clostridium beijerinckii* by Bogin *et al.* revealed that significant protein stabilization could be achieved by extending the intersubunit interactions of a secondary ADH.[14]

In the present study, we further investigated the relevance of intersubunit associations to the stability of multimeric ADHs.

This study is part of an ongoing study on the molecular basis of thermal stability in a model system comprising three functionally related, highly homologous, medium-chain, NADP(H)-linked ADHs (EC 1.1.1.2.), all showing similar substrate specificity.[14,15] Specifically we are studying the ADHs from *Thermoanaerobacter brockii* (TbADH),[16] the mesophilic bacterium *C. beijerinckii* (CbADH),[16] and from the protozoan parasite *Entamoeba histolytica* (EhADH1).[15] All three enzymes reversibly catalyze the oxidation of secondary alcohols to the corresponding ketones using $NADP^+$ as cofactor. We isolated and characterized TbADH and cloned, sequenced, and overexpressed the structural *adh* genes from *T. brockii*,[16] *C. beijerinckii*,[16] and *E. histolytica*[17] in *Escherichia coli*. Amino acid sequence alignments of the three ADHs (Fig. 1) revealed high-sequence conservation among the three members of this enzyme family—75% identity between TbADH and CBADH, 66% identity between EhADH1 and TBADH, and 62% identity between EhADH1 and CbADH.[20] Interestingly, the proline residues are more highly conserved than other amino acids in the sequence, with all 13 proline residues of the mesophilic CbADH being present in TbADH, of which 12 are also present in EhADH1.[20] Despite their high degree of sequence homology, the enzymes differ greatly in thermal stability with $T_{1/2}$ values of CbADH < EhADH1 < TbADH (64.5, 77.5, 93.8°C, respectively).[14,16,20] The thermal denaturation process is irreversible, followed by precipitation of the inactive denatured enzyme.

An examination of the crystal structures of TbADH, CbADH,[18] and EhADH1[19] at the respective resolutions of 2.50, 2.05, and 1.81 Å revealed that the three enzymes are homotetramers comprising 38 kDa subunits sharing identical catalytic Zn-binding sites.

Further analysis of the crystal structures of holo-TbADH (PDB entry 1YKF) revealed several features that might account for high thermal stability of TbADH.[18] One element that appears to be crucial is Pro275, which is located at the center of the dimerization interface between two monomers, increasing (a) the rigidity of the resulting structural element and (b) the stability of subunit interactions in the resulting dimmers.[18] In the less thermostable EhADH1, position 275 is occupied by Asp.

We previously reported that the substitution of Gln100 in the mesophilic CbADH, located at the structural lobe at the dimer–dimer interface, with Pro of EhADH1 enhanced the stability of that enzyme.[21]

Here, we report that a single substitution of the Pro275 of TbADH for Asp in EhADH1 (D275P-EhADH1) significantly enhanced the thermal stability of the latter enzyme, whereas the reverse substitution in TbADH (P275D-TbADH) reduced the thermal stability of the thermophilic enzyme. Our findings, based on examination of 3D structures of mutated enzymes, suggested that a Pro substitution at this position stabilizes the protein by increasing the number of hydrophobic interactions and by reducing the flexibility at the dimerization interface.

MATERIALS AND METHODS

Site-directed mutagenesis

The enzymes for DNA cloning, sequencing, and amplification were purchased from Amersham (Buckinghamshire, England), New England Biolabs (Beverly, MA), Fermentas MBI (Vilnius, Lithuania), and Promega (Madison, WI). Oligonucleotides for cloning, sequencing, and site-directed mutagenesis (SDM) of the *T. brockii, E. histolytica*, and *C. beijerinckii adh* genes were synthesized by the WIS Chemical Synthesis Laboratory. All other chemicals were of analytical grade. The genes encoding TbADH and EhADH1 were constructed and expressed according to Peretz *et al.*[16] using the plasmids $pBSP80^{TbADH}$, and $pBSP80^{EhADH1}$ as templates for generating the recombinant plasmids coding for the respective mutants P275D-TbADH, and D275P-EhADH1. SDM was performed using the QuikChange XL SDM kit of stratagene (La Jolla, CA). The mutations were verified by DNA sequencing of the corresponding plasmids. The forward primers used for generating the mutants are listed below, with the exchanged bases *italicized*. The sequences of the corresponding reverse primers were complementary to the forward primers.

For P275D-TbADH: 5′-GGCGAAGGAGAGGTTTTGG***A***TGTTCCTCGTCTTGAATGG-3′

For D275P-EhADH1: 5′-GAGAAGGAGATAATATT***CC***TATTCCAAGAAGTGAATGGGG-3′

Expression and purification of recombinant enzymes

All recombinant plasmids bearing TbADH, EhADH1, and their mutated variants were transformed into *E. coli*

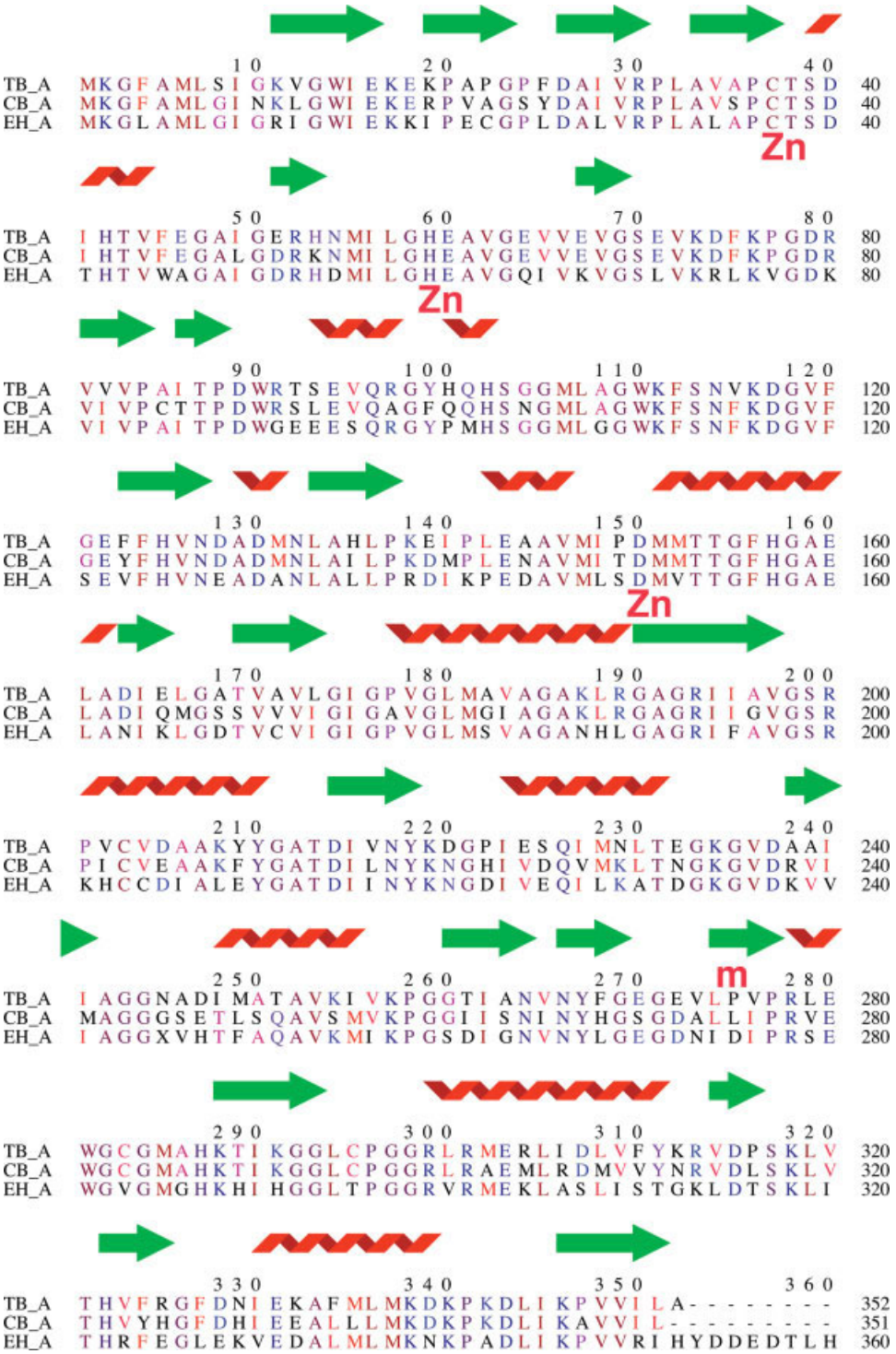

Figure 1

Structure-based sequence alignment of ADHs from Thermoanaerobacter brockii *(TbADH, TB[18]),* Clostridium beijerinckii *(CbADH, CB[18]) and* Entamoeba histolytica *(EhADH, EH[19]). The secondary structure elements are shown above the sequences with twisted rods for α-helices and arrows for β-strands. The mutagenesis site (m) and the metal ligand residues (Zn) are depicted above and below the sequence, respectively. The figure was prepared with INDONESIA program package http://alpha2.bmc.uu.se/~dermis/.*

strain TG-1, and the recombinant proteins were purified according to a modification of a procedure described by Peretz *et al.*[16] Briefly, the transformed cells were cultured for 17 h in 2YT with zinc chloride (10 μ*M*) and ampicillin (100 mg L^{-1}) at 37°C, harvested by centrifugation for 20 min at 8000*g* (4°C), and resuspended in buffer A (25 m*M* Tris-HCl, pH 7.3; 0.1 m*M* DTT, 0.1 m*M* EDTA, 0.1 m*M* benzamidine, 0.02% sodium azide, and 10% glycerol). The cells were disrupted for 5 min by pulsed sonication (Branson Sonifier 450) using a rosette cup immersed in an ice bath and then centrifuged (23,000*g* for 30 min) to remove cell debris. The supernatant was then heat-treated for 3 min at 65°C and recentrifuged for 15 min at 12,000*g*. The clear supernatant was applied onto a DEAE-52-cellulose column (10 × 2.5 cm^2), preequilibrated with buffer A at 4°C. The column was extensively washed with buffer A until the eluate contained no detectable protein according to the method of Bradford.[22] The proteins were eluted from the column with buffer A containing 0.1*M* NaCl, and the enzymatically active fractions were pooled and applied onto a short Red Sepharose column (12 × 2.5 cm^2) (Pharmacia, Uppsala, Sweden). The purified recombinant enzymes eluted from the Red Sepharose column in a linear gradient of NaCl at concentration ranges of 0.1–1*M* for TbADH, and 50–250 m*M* for EhADH1 in buffer A. The fractions containing ADH activity were collected, concentrated by ultrafiltration (Amicon YM-30), and stored at 4°C. All mutant enzymes used in this study were purified to homogeneity, as judged by Coomassie Brilliant Blue staining of SDS-polyacrylamide gel electrophoresis (PAGE) gels.

Enzyme activity assay

The catalytic activity of ADH at 40°C was measured by following the reduction of $NADP^+$ (and the formation of NADPH), monitored at 340 nm (ε_{340} = 6.2 mM^{-1} cm^{-1}). The standard assay mixture contained 150 m*M* 2-butanol, 0.5 m*M* $NADP^+$, and 100 m*M* Tris-HCl (pH 9.0) in a total volume of 1 mL. One unit of ADH is defined as the amount of enzyme that catalyzes the oxidation of 1 μmole of 2-butanol min^{-1} at 40°C under the initial velocity at the above-mentioned conditions. Kinetic parameters were measured and calculated using a Beckman DU-7500 spectrophotometer equipped with a Multicomponent/SCA/Kinetics Plus software package and a thermostatted circulating water bath. The K_m values for 2-butanol were determined using increasing concentrations of alcohol (0.1–100 m*M*) and enzyme (5–120 n*M*) with 0.5 m*M* $NADP^+$ in 100 m*M* Tris-HCl (pH 9.0). The values represent the average of three experiments; individual measurements were within 10% of the quoted mean.

Circular dichroism

Far-UV (200–260 nm) CD spectra were performed at a temperature range of 30–110°C with an average increase in temperature of 1°C min^{-1}, using an Aviv spectrophotometer, Model 202. Scans were performed every 4°C using ~1.25 μ*M* (0.5 mg mL^{-1}) protein in 25 m*M* Na/K phosphate buffer, pH 6.8, in quartz cells and with a light path of 0.1 cm. Data (mdeg versus wavelength) were collected every nanometer with an averaging time of 2 s. The background CD signal for each analysis, determined in a single scan using buffer alone at 25°C, was subtracted from each scan and was temperature-independent. The decrease in CD signal with increase of temperature was evaluated at the local minima of 218 nm and further normalized by subtracting from each wavelength the lowest signal observed at that particular wavelength.

Thermal inactivation ($T_{1/2}^{60min}$ and $T_{1/2}^{CD}$)

The thermal stability of the ADHs was determined by monitoring the residual enzymatic activity after 60 min incubation in 25 m*M* Na/K phosphate buffer (pH 6.8) at increasing temperatures. $T_{1/2}^{60min}$ is the temperature at which 50% of the enzymatic activity is lost after 1-h incubation, interpolated from a plot of the residual enzymatic activity versus temperature. $T_{1/2}^{CD}$ is the temperature at which 50% of the original CD signal at 218 nm is lost upon heating the protein sample between 30°C and 98°C (between 30 and 110°C for TbADH), with an average increase in temperature of 1°C min^{-1}. The value is the mean of three experiments; individual measurements were within 5% of the quoted mean.

Analytical procedures

DNA sequencing was performed on an Applied Biosystems Model 373A DNA sequencer using the dideoxy method according to Sanger and Coulson[23] and appropriate primers. SDS-PAGE was performed on 12% slab gels and 5% stacking gels according to Laemmli[24] (Bio-Rad MiniProtean II system) and stained with Coomassie Brilliant Blue. Protein concentrations were determined according to Bradford,[22] using bovine serum albumin as standard. The estimated molecular weight of the recombinant enzymes was determined by size exclusion chromatography on a column of Superdex S-200.

Crystallization, data collection, and refinement

D275P–EhADH1

Crystals of D275P–EhADH1 were grown using the hanging-drop vapor-diffusion method at 20°C. In the final conditions for crystallization, 1 μL of apo-D275P–EhADH1 stock solution [8 mg mL^{-1} protein, 25 m*M* Tris-HCl, 50 m*M* NaCl, 0.1 m*M* DTT, 50 m*M* $ZnCl_2$ (pH 7.5)] was mixed with 1 μL of reservoir solution [25% (v/v) PEG 600, 100 m*M* calcium acetate, 200 m*M*

cacodylate (pH 6.4)]. Prior to data collection, crystals were soaked for several hours in cryo-protectant that contained mother liquor plus 30% ethylene glycol. Diffraction data from D275P–EhADH1 crystals were measured using synchrotron radiation (ID14-2 beam line at ESRF, Grenoble, France). An ADSC Q4 detector and X-ray radiation of 0.933 Å wavelength were used. Diffraction data to resolution 1.77 Å were collected in 0.5° oscillation frames and processed with HKL2000.[25] Crystals formed in space group C2, with cell constants a = 149.93 Å, b = 144.10 Å, c = 80.08 Å, β = 121.44°. The structure was solved by MOLREP[26] using the coordinates of *E. histolytica* ADH (1Y9A, Protein Data Bank). Data collection and refinement statistics are presented in Table I. All steps of atomic refinement were carried out with the program REFMAC.[27] Map display and model rebuilding were performed using the program COOT,[28] and model inspection using WHATIF[29] and PROCHECK.[30]

P275D–TbADH

Crystals of P275D–TbADH were grown using the hanging-drop vapor-diffusion method at 20°C. In the final conditions for crystallization, 1 μL of holo-P275D-TbADH stock solution [10 mg mL^{-1} protein, 2 m*M* $NADP^+$, 25 m*M* Tris-HCl, 50 m*M* NaCl, 0.1 m*M* DTT, 50 m*M* $ZnCl_2$ (pH 7.5)] was mixed with 1 μL reservoir solution [16% (w/v) PEG 4K, 50 m*M* NaCl, 50 m*M* Tris-HCl (pH 8.3)]. Prior to data collection, crystals were soaked for several hours in cryo-protectant that contained 60% of the mother liquor plus 25% ethylene glycol. A complete data set from a single crystal of holo P275D-TbADH was collected at 100°K on a Rigaku R-AXIS IV++ imaging plate area detector using a Rigaku RU-H3R rotating anode operated at 5 kW and Osmic multilayer X-ray focusing mirrors.

Diffraction data were integrated, scaled, and reduced using the HKL program package.[25] Crystals formed in space group $P2_12_12_1$, with cell constants a = 79.60 Å, b = 125.01 Å, and c = 167.11 Å. The crystals contain one tetramer in the asymmetric unit cell with Vm of 3.18 $Å^3$/Dalton and diffracted to 2.8 Å resolution. The structure was solved by molecular replacement using the program PHASER[31] by using the refined structure of apo-TbADH (1YKF, Protein Data Bank) as a model. Data collection and refinement statistics are presented in Table I.

All steps of atomic refinement were carried out with the program CNS.[32] Map display and model rebuilding were performed using the program O,[33] and model inspection using WHATIF[29] and PROCHECK.[30]

The PDB accession codes for P275D–TbADH and D275P-EhADH1 are 2NVB and 2OUI, respectively. The figures were created using the program PyMOL (DeLano Scientific LLC).

Table I
Data Collection and Refinement Statistics of D275P-EhADH1 and P275D-TbADH

	D275P-EhADH1	P275D-TbADH
Crystal data		
Source	ESRF, ID14-2	Rigaku RU-H3R
Space group	C2	$P2_12_12_1$
Temperature	100K	100K
Unit-cell parameters	a = 149.93 Å, b = 144.10 Å, c = 80.08 Å, β = 121.44°	a = 70.60 Å, b = 125.01 Å, c = 167.11 Å
Internal scaling		
Resolution (Å)	50.0–1.77 (1.82–1.77)	40.0–2.80 (2.9–2.8)
Reflections measured	516941	270326
Unique reflections	135908 (6758)	40410 (3894)
Completeness (%)	98.90 (98.50)	96.50 (94.0)
$I/\sigma(I)$ (average)	19.4 (1.56)	12 (2.43)
R_{sym}	0.060	0.085
Model refinement		
Resolution range (Å)	50.0–1.77 (1.82–1.77)	39.6–2.8 (2.98–2.8)
Molecules AU	4	4
No. protein residues	1440	1408
Wilson B factor $Å^2$	18.49	22.07
Overall B factor $Å^2$	28.05	33.8
R_{cryst}	0.148 (0.221)	0.217 (0.317)
R_{free} 5% of data	0.178 (0.286)	0.278 (0.363)
Geometry		
RMS bonds (Å)	0.014	0.008
RMS bonds angles (°)	1.503	1.5
RMS planar groups (°)	0.009	0.005
Estimated coordinate error (Å)		
Low res. cutoff	5.0	5.0
Estimated error	0.07	0.36
Ramachandran statistics (%)		
Most favored	90.5	84.0
Additional allowed	9.5	15.3
Generously allowed	0.0	0.7
Disallowed regions	0.0	0.0

$R_{sym} = \sum|\langle I_{hkl}\rangle - I_{hkl}|/|I_{hkl}|$, where $\langle I_{hkl}\rangle$ is the average intensity over symmetry-related reflections and I_{hkl} is the observed intensity.
$R_{cryst} = \sum||F_o|-|F_c||/\sum|F_o|$, where F_o denotes the observed structure factor amplitude and F_c the structure factor calculated from the model.
R_{free} is for 5% of randomly chosen reflections excluded from the refinement.

RESULTS AND DISCUSSION

Site-directed mutagenesis—molecular and enzymatic properties of the mutant enzymes

The tetrameric ADHs studied here are dimers of dimers, in which subunits A and B (or C and D) compose the main horse liver-ADH-like dimer, and two such dimers (AB and CD) associate through subunits A and C (or B and D), and A and D (or B and C) to form the tetramer [Fig. 2(a)].

In the extreme thermophilic TbADH, Pro275 is located in the middle of an extended stretch of amino acid residues that are involved in the dimerization of the A-B dimers.[19] In the thermophilic EhADH1, residue 275 is Asp. To assess the contribution of Pro275 to the thermostability of the enzymes, we used SDM to replace Pro275

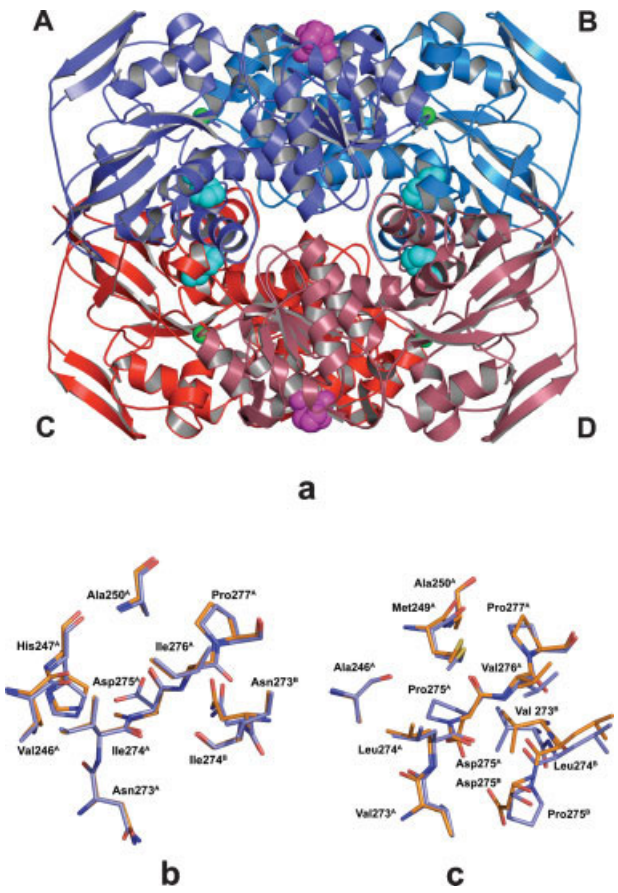

Figure 2

*(**a**) Ribbon diagram of the TbADH tetramer. Subunits are represented in different colors. Pro residues, depicted in ball representation, are colored magenta (Pro275) and cyan (Pro100). The active site Zn is colored green. (**b**) Superimposition of the structures of the wild-type apo-EhADH1 (colored orange) and the apo D275P-EhADH1 mutant (colored green). Residues within a sphere of a 4-Å radius of the mutation are shown (the superscript refers to the subunit). (**c**) Superimposition of the structures of the wild-type holo-TbADH (colored green) and the holo P275D-TbADH mutant (colored orange). Residues within a sphere of a 4-Å radius of the mutation are shown (the superscript refers to the subunit).*

of TbADH with Asp (as occurs in EhADH1) and, conversely, to replace Asp275 of EhADH1 with Pro, forming the respective mutant enzyme P275D-TbADH.

The purified recombinant enzymes, characterized by size-exclusion chromatography and SDS-PAGE, displayed the apparent molecular weights of 160 kDa per tetramer and 38 kDa per monomer, similar to those of the wild-type enzymes (data not shown).[15]

Table II shows the kinetic properties of the enzymatic activity of TbADH, EhADH1, and their mutants at 40°C, using 2-butanol as substrate. The similarity of the K_m values of the mutants and their enzymatic efficiency (K_{cat}/K_m) to those of native ADHs indicates that neither the binding nor the catalytic efficiency of the enzymes was severely affected by the mutations. Indeed, the mutation of residue 275 in ADH is relatively remote from the active site of the enzyme,[19] and any structural change that might have resulted from these mutations presumably did not perturb the active site.

Table II
Kinetic Parameters of the ADHs[a]

ADHs	K_m (m*M*)	K_{cat} (min^{-1})	K_{cat}/K_m (mM^{-1} min^{-1})
TbADH	3.1	1724	556
P275D-TbADH	4.9	1000	204
EhADH1	0.74	3025	4088
D275P-EhADH1	0.95	5052	5318

Enzymatic activity was measured by monitoring the formation of NADPH at 340 nm. K_m values for 2-butanol were determined with varying concentrations of 2-butanol (0.1−100 m*M*), enzyme (5−120 n*M*) and 0.5 m*M* $NADP^+$ in 100 m*M* Tris-HCl (pH 9) in a total volume of 1 mL, in triplicates at 40°C. Values are the averages of two experiments and the individual measurements were within 10% of the quoted mean.
[a]Alcohol dehydrogenases.

Thermal stability

The $T_{1/2}^{60min}$ and $T_{1/2}^{CD}$ values of the mutants are presented in Table III and in Figures 3 and 4, respectively. Replacing Asp275 with Pro significantly enhanced the thermal stability of EhADH1: $\Delta T_{1/2}^{60min} = +9.3$°C, $\Delta T_{1/2}^{CD} = +10$°C. As expected, the reverse mutation in the thermophilic TbADH—namely, replacing Pro275 with Asp of EhADH1—reduced the thermal stability of the enzyme: $\Delta T_{1/2}^{60min} = -13.8$°C, $\Delta T_{1/2}^{CD} = -18.8$°C.

These findings demonstrate that a single proline substitution is responsible for the huge differences in the thermal stability of two homologous ADHs, and highlight the important role played by proline residues in preserving protein stability. Indeed it has been recently shown that substitution by proline at strategic positions could significantly stabilize the protein. For example Prajapati *et al.* have stabilized three different proteins—LIVBP, leucine–isoleucine–valine binding protein; MBP,

Table III
Thermal Parameters of the ADHs[a]

ADHs	$T_{1/2}^{60min}$ (°C)[b]	$\Delta T_{1/2}^{60min}$ (°C)[c]	$T_{1/2}^{CD}$ (°C)[b]	$\Delta T_{1/2}^{CD}$ (°C)[c]
TbADH	93.8		93.8	
P275D-TbADH	75	−18.8	80	−13.8
EhADH1	77.5		80	
D275P-EhADH1	86.8	+9.3	90	+10

[a]Alcohol dehydrogenases
[b]$T_{1/2}^{60min}$ is the temperature at which 50% of the enzymatic activity is lost after 1-h incubation, interpolated from a plot of the residual enzymatic activity versus temperature. $T_{1/2}^{CD}$ is the temperature at which 50% of the original CD signal at 218 nm is lost upon heating the protein sample between 30° and 98°C (30 and 110°C for TbADH), with an average increase in temperature at 1°C/min.
[c]Relative to the wild type enzyme.

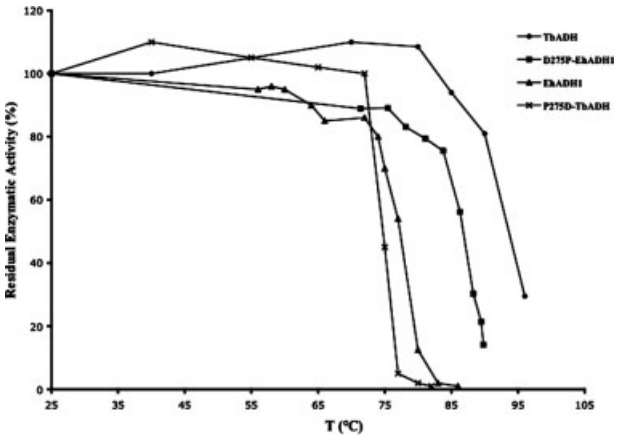

Figure 3

The effect of the mutations on the thermal stability of the enzymatic activity of the ADHs. The thermal stability of the enzymes was determined by monitoring their residual enzymatic activity after 60-min incubation at varying temperatures. Enzymatic activity was assayed by spectrophotometric analysis of NADPH formation at 340 nm (as described under materials and methods). Values are expressed as the averages of at least three experiments.

maltose binding protein; and Trx, *E. coli* thioredoxin, by carefully designed proline substitutions.[34] Kelch and Agard have compared the structures of homologous mesophilic and thermophilic α-lytic proteases (αLP) and suggested that the kinetic stability of the thermophilic αLP is due to strategic placement of prolines at loop regions.[35]

Structural considerations

We crystallized the D275P-EhADH1 and P275D-TbADH proteins and solved the 3D structures of D275P-EhADH1 and P275D-TbADH by X-ray crystallography to resolutions of 1.7 and 2.8 Å, respectively. A comparison of the 3D structures of the mutants with the 3D structures of their native ADHs showed that within both pairs of ADHs (EhADH1 and TbADH), the Cα chains of both the native and the Pro275 mutant enzymes were almost identical (r.m.s. difference in Cα of 0.271 Å between the monomer of EhADH1 and the monomer of D275P-EhADH1, and 0.4 Å between the monomer of TbADH and the monomer of P275D-TbADH). The differences between the wild types and mutants are confined to the site of the mutation, where the Asp to Pro mutation removed a long-distance ion pair between Oδ1 of Asp275 and Nε2 of His247 (distance = 4.2 Å) from EhADH1.

In both TbADH and EhADH1, residue 275 is located at the middle of a stretch (residues 268–278) through which the two subunits A (or C) and B (or D) interact via hydrophobic interactions and hydrogen bonds. The α-helix αF (residues 245–254) provides support for the stretch through additional hydrophobic interactions between it and other parts of the cofactor-binding domain of the same subunit.[18,19]

In the native EhADH1 enzyme, a hydrophobic interaction occurs between the Cβ Asp275 and the Cβ of Asn273 from the subunit B (distance = 3.8 Å). The Asp⇑Pro mutation introduced two additional CH_2 groups, Cγ and Cδ of Pro275 into the mutation site [Fig. 2(b)], thereby optimizing the van der Waals interactions and the hydrophobicity at the mutation region.

We suggest that the extensive stabilization of the D275P-EhADH mutant was brought about by (a) increasing the rigidity of the dimerization interface and increasing the van der Waals interactions and (b) the hydrophobic effect brought about via the burial of two additional methylene groups at the nearby hydrophobic surrounding.

Similarly in P275D-TbADH, the methylenes Cγ and Cδ of Pro275 were eliminated from the mutation site. In the wild type TbADH, in addition to the hydrophobic interaction between the Cβ of Pro275 and the Cβ, Cγ1, and Cγ2 of Val273 from the subunit B (distance = 3.7, 3.8, and 4.2 Å, respectively), the Cδ of Pro275 approaches the Cβ of Ala246, Cβ of Met249 and Cβ of Leu274 (∼4.4, 4.9, and 4.1 Å, respectively) [Fig. 2(c)].

In addition, an unfavorable electrostatic interaction was created between Oδ1 of the carboxylic group of the side chain of Asp275 of chain A (or C) with the Oδ1 of the carboxylic group of the side chain of Asp275 of chain B (or D), (distanced 2.59 Å) [Fig. 2(c)]. We therefore concluded that the destabilization of P275D-TbADH is due to a combination of (a) the decreased rigidity and

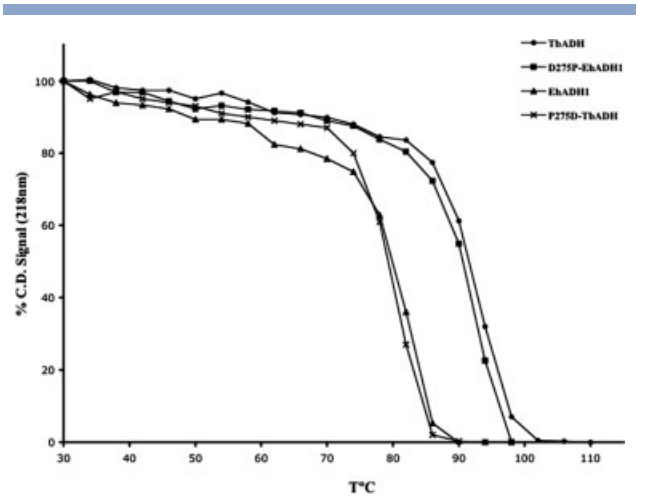

Figure 4

The effect of the mutations on the thermal stability of the secondary structure of the ADHs. Thermal stability of the enzymes was determined by monitoring the loss of their CD signal at 218 nm upon heating (as described under materials and methods).

hampering of stabilizing van der Waals and hydrophobic interactions by the substitution of Pro275 and (b) unfavorable electrostatic interactions.

Previously we reported that substituting Ile275 of the mesophilic CbADH with the Pro of TbADH destabilized the enzyme. Nevertheless, combining this mutation with a second substitution Ala273⇑Ile considerably stabilized the protein by adjusting the hydrophobic interactions and the rigidity at that region.[20]

Similarly, by increasing the rigidity and optimizing the hydrophobic interactions in the present study, we substantially stabilized the moderate thermophile EhADH1 by a single Pro substitution at a strategic region at the centre of the dimerization interface, which is crucial for the maintenance of the quaternary structure of the enzyme.

Finally, our study demonstrates that a single amino acid difference, located at a structurally strategic region of a protein molecule, could account for a huge difference in the thermal stability between homologous oligomeric proteins.

ACKNOWLEDGMENTS

We thank Dr. Virginia Buchner for helpful discussions and suggestions during manuscript preparation. The three-dimensional structure of P275D-TbADH was solved at the Israel Structural Proteomics Center (ISPC). We thankfully acknowledge the ESRF for synchrotron beam time and the staff scientists of the ID-14 station cluster for their assistance.

REFERENCES

1. Fitter J. Structural and dynamical features contributing to thermostability in alpha-amylases. Cell Mol Life Sci 2005;62:1925–1937.
2. Siddiqui KS, Cavicchioli R. Cold-adapted enzymes. Annu Rev Biochem 2006;75:403–433.
3. Jaenicke R. Stability and stabilization of globular proteins in solution. J Biotechnol 2000;79:193–203.
4. Unsworth LD, van der Oost J, Koutsopoulos S. Hyperthermophilic enzymes—stability, activity and implementation strategies for high temperature applications. FEBS J 2007;274:4044–4056.
5. Zhou XX, Wang YB, Pan YJ, Li WF. Differences in amino acids composition and coupling patterns between mesophilic and thermophilic proteins. Amino Acids (Published online ahead of print: August 21, 2007).
6. Wiseman RL, Green NS, Kelly JW. Kinetic stabilization of an oligomeric protein under physiological conditions demonstrated by a lack of subunit exchange: implications for transthyretin amyloidosis. Biochemistry 2005;44:9265–9274.
7. Mitra N, Srinivas VR, Ramya TN, Ahmad N, Reddy GB, Surolia A. Conformational stability of legume lectins reflect their different modes of quaternary association: solvent denaturation studies on concanavalin A and winged bean acidic agglutinin. Biochemistry 2002;41:9256–9263.
8. Bjork A, Dalhus B, Mantzilas D, Eijsink VG, Sirevag R. Stabilization of a tetrameric malate dehydrogenase by introduction of a disulfide bridge at the dimer-dimer interface. J Mol Biol 2003;334:811–821.
9. Nakka M, Iyer RB, Bachas LG. Intersubunit disulfide interactions play a critical role in maintaining the thermostability of glucose-6-phosphate dehydrogenase from the hyperthermophilic bacterium *Aquifex aeolicus*. Protein J 2006;25:17–21.
10. Stroppolo ME, Malvezzi-Campeggi F, Mei G, Rosato N, Desideri A. Role of the tertiary and quaternary structures in the stability of dimeric copper, zinc superoxide dismutases. Arch Biochem Biophys 2000;377:215–218.
11. Esposito L, Sica F, Raia CA, Giordano A, Rossi M, Mazzarella L, Zagari A. Crystal structure of the alcohol dehydrogenase from the hyperthermophilic archaeon *Sulfolobus solfataricus* at 1.85 A resolution. J Mol Biol 2002;318:463–477.
12. Guy JE, Isupov MN, Littlechild JA. The structure of an alcohol dehydrogenase from the hyperthermophilic archaeon *Aeropyrum pernix*. J Mol Biol 2003;331:1041–1051.
13. Levin I, Meiri G, Peretz M, Burstein Y, Frolow F. The ternary complex of *Pseudomonas aeruginosa* alcohol dehydrogenase with NADH and ethylene glycol. Protein Sci 2004;13:1547–1556.
14. Bogin O, Levin I, Hacham Y, Tel-Or S, Peretz M, Frolow F, Burstein Y. Structural basis for the enhanced thermal stability of alcohol dehydrogenase mutants from the mesophilic bacterium *Clostridium beijerinckii*: contribution of salt bridging. Protein Sci 2002;11:2561–2574.
15. Kumar A, Shen PS, Descoteaux S, Pohl J, Bailey G, Samuelson J. Cloning and expression of an NADP(+)-dependent alcohol dehydrogenase gene of *Entamoeba histolytica*. Proc Natl Acad Sci USA 1992;89:10188–10192.
16. Peretz M, Bogin O, Tel-Or S, Cohen A, Li G, Chen J-S, Burstein Y. Molecular cloning, nucleotide sequencing, and expression of genes encoding alcohol dehydrogenases from the thermophile *Thermoanaerobacter brockii* and the mesophile *Clostridium beijerinckii*. Anaerobe 1997;3:259–270.
17. Shimon LJ, Peretz M, Goihberg E, Burstein Y, Frolow F. Thermophilic alcohol dehydrogenase from the mesophile *Entamoeba histolytica*: crystallization and preliminary X-ray characterization. Acta Crystallogr D Biol Crystallogr 2002;58 (Part 3):546–548.
18. Korkhin Y, Kalb AJ, Peretz M, Bogin O, Burstein Y, Frolow F. Oligomeric integrity—the structural key to thermal stability in bacterial alcohol dehydrogenases. Protein Sci 1999;8:1241–1249.
19. Shimon LJ, Goihberg E, Peretz M, Burstein Y, Frolow F. Structure of alcohol dehydrogenase from *Entamoeba histolytica*. Acta Crystallogr D Biol Crystallogr 2006;62 (Part 5):541–547.
20. Bogin O, Peretz M, Hacham Y, Korkhin Y, Frolow F, Kalb AJ, Burstein Y. Enhanced thermal stability of *Clostridium beijerinckii* alcohol dehydrogenase after strategic substitution of amino acid residues with prolines from the homologous thermophilic *Thermoanaerobacter brockii* alcohol dehydrogenase. Protein Sci 1998;7:1156–1163.
21. Goihberg E, Dym O, Tel-Or S, Levin I, Peretz M, Burstein Y. A single proline substitution is critical for the thermostabilization of *Clostridium beijerinckii* alcohol dehydrogenase. Proteins 2007;66:196–204.
22. Bradford MM. A rapid and sensitive method for the quantitation of microgram quantities of protein utilizing the principle of protein-dye binding. Anal Biochem 1976;72:248–254.
23. Sanger F, Coulson AR. A rapid method for determining sequences in DNA by primed synthesis with DNA polymerase. J Mol Biol 1975;94:441–448.
24. Laemmli UK. Cleavage of structural proteins during the assembly of the head of bacteriophage T4. Nature 1970;227:680–685.
25. Otwinowski Z, Minor W. Processing of X-ray diffraction data collected in oscillation mode. Methods Enzymol A 1997;276:307–326.
26. Vagin A, Teplyakov A. MOLREP: an automated program for molecular replacement. J Appl Crystallogr 1997;30:1022–1025.
27. Murshudov GN, Vagin AA, Dodson EJ. Refinement of macromolecular structures by the maximum-likelihood method. Acta Crystallogr D Biol Crystallogr 1997;53 (Part 3):240–255.
28. Emsley P, Cowtan K. Coot: model-building tools for molecular graphics. Acta Crystallogr D Biol Crystallogr 2004;60 (Part 12):2126–2132.

29. Vriend G. WHAT IF: a molecular modeling and drug design program. J Mol Graph 1990;8:52–56, 29.
30. Laskowski RA, Macarthur MW, Moss DS, Thornton JM. Procheck—a program to check the stereochemical quality of protein structures. J Appl Crystallogr 1993;26:283–291.
31. Storoni LC, McCoy AJ, Read RJ. Likelihood-enhanced fast rotation functions. Acta Crystallogr D Biol Crystallogr 2004;60 (Part 3):432–438.
32. Brunger AT, Adams PD, Clore GM, DeLano WL, Gros P, Grosse-Kunstleve RW, Jiang JS, Kuszewski J, Nilges M, Pannu NS, Read RJ, Rice LM, Simonson T, Warren GL. Crystallography and NMR system: a new software suite for macromolecular structure determination. Acta Crystallogr D Biol Crystallogr 1998;54:905–921.
33. Jones TA, Kjeldgaard M. Electron-density map interpretation. Methods Enzymol B 1997;277:173–208.
34. Prajapati RS, Das M, Sreeramulu S, Sirajuddin M, Srinivasan S, Krishnamurthy V, Ranjani R, Ramakrishnan C, Varadarajan R. Thermodynamic effects of proline introduction on protein stability. Proteins 2007;66:480–491.
35. Kelch BA, Agard DA. Mesophile versus thermophile: insights into the structural mechanisms of kinetic stability. J Mol Biol 2007; 370:784–795.